Biosensors and Bioelectronics 142 (2019) 111537

Contents lists available at ScienceDirect

Biosensors and Bioelectronics

journal homepage: www.elsevier.com/locate/bios

# Ratiometric electrochemical biosensor based on Exo III-Assisted recycling amplification for the detection of CAG trinucleotide repeats

Yalan Liu, Zhiqi Ge, Meijun Chen, Hanping He*, Xiuhua Zhang, Shengfu Wang

*Hubei Collaborative Innovation Center for Advanced Organic Chemical Materials & Ministry of Education Key Laboratory for the Synthesis and Application of Organic Functional Molecules, Hubei University, Youyi Road 368, Wuchang, Wuhan, Hubei, 430062, PR China*

ARTICLE INFO

*Keywords:*
Electrochemical sensors
Trinucleotide repeat
Exo III-Assisted recycling
Ratiometric technique
Graphene

ABSTRACT

Electrochemical detection of specific nucleic acid sequence remains a hot topic in current bioanalytical research. Here, a novel ratiometric electrochemical biosensor based on Exo III-assisted recycling amplification and graphene-modified electrode was fabricated for quantitative detection of trinucleotide repeat sequence $d(CAG)_n$. The double-signals used are the hairpin DNAs labeled with ferrocene and methylene blue respectively as report DNAs, which can hybridize to target DNA. The hybridized DNA was digested by Exo III, resulting in the release of target and report fragments. The graphene-modified electrode can selectively adsorb the released report fragments to generate double electrochemical signals. The signal ratio (F/M) of ferrocene and methylene blue was used to determine the repeat length accurately: a linear relationship was found between F/M and numbers of repeats (n), F/M = 0.061 n + 1.97, with a correlation coefficient of 0.992. Moreover, any electrochemical signal can be used to test repeat concentration with detection limit of 0.22 pM. Therefore, this novel ratiometric electrochemical biosensor provided a reliable and efficient method for the analysis of $d(CAG)_n$ trinucleotide repeat and a potential simplified clinical tool for neurodegenerative diseases.

## 1. Introduction

Trinucleotide repeat (TNR) disease is caused by repeated unstable expansions in a particular gene by any group of trinucleotide, such as CCG, CAG, AAG, CTG, GCG (Fu et al., 1991; La Spada et al., 1991; Stevens et al., 2013). As the length of the repetition increases, the chances get the disease increases accordingly (Kremer et al., 1994; Ranen et al., 1995). For example, an increase in the CAG trinucleotide repeat leads to the Huntington's disease. Abnormal expression of the GAA trinucleotide repeat causes Friedreich's ataxia, which is present in the 5′ untranslated region of the FMR1 gene. The CGG trinucleotide repeat is associated with fragile X syndrome (Dürr et al., 1996; Evansgalea et al., 2013; López Castel et al., 2010; Lin et al., 2015; Mirkin, 2007; Sutherland and Richards, 1995). Furthermore, a common feature of the diseases caused by amplification of trinucleotide repeat is the phenomenon of the hereditary prevalence which refers to the presence of certain genetic diseases for several generations: in this case, their associated symptoms are increasingly severe generation, while their onset time is one generation earlier than one generation (Lange and Mcinnis, 2002). Therefore, early diagnosis of trinucleotide repeat disease is particularly crucial.

The scientific community generally believes that extensible repeat sequences have abnormal structural properties. It has found that sequences such as $d(CGG)_n$, $d(CTG)_n$, $d(CAG)_n$, can form a sliding hairpin-like structure consisting of a composition of the Watson-Crick base pairs and the non-Watson-Crick base pairs (Mitchell et al., 1995; Suen et al., 1999; Yu et al., 1995). Due to its structural characteristics, the rapid diagnostic process is rather complex. Currently, the detection of trinucleotide repeat relies mainly on traditional sequencing techniques, such as gel electrophoresis, southern blotting, and PCR amplification (Fu et al., 1991; Snow et al., 1993; Zühlke et al., 2015). However, these methods have some limitations, such as the need of professional technology for complex operations, and expensive equipment. Recently, developing rapid and simple medical diagnosis methods and devices have attracted increasing attention. Compared to other methods, electrochemical method exhibits its unique advantages, including simple operation, low power consumption, and high sensitivity (He et al., 2014; Kannan et al., 2011; Lin et al., 2015). However, few studies on the detection of trinucleotide repeat by the electrochemical method are available in the literature. Emil Palecek and coworkers used nucleic acid hybridization to study the electrochemical detection of TTC and GAA trinucleotide repeat PCR products(Fojta et al. 2004, 2005). In previous work, we had studied some electrochemical methods, including bifunctional electrochemical probes, magnetic separation

* Corresponding author.
*E-mail address:* hehanping@hubu.edu.cn (H. He).

https://doi.org/10.1016/j.bios.2019.111537
Received 24 April 2019; Received in revised form 11 July 2019; Accepted 24 July 2019
Available online 25 July 2019
0956-5663/ 

technology, and impedance spectroscopy, to detect trinucleotide repeats (He et al. 2013, 2014; Li et al., 2017c; Liu et al., 2018; Zhu et al., 2017).

In order to improve stability and sensitivity of the electrochemical signal, several signal amplification techniques have been used in the DNA detection, such as signal amplification induced by Exo III-assisted cycle, DNA polymerase, hybridization chain reaction, toehold-mediated strand displacement reaction, and rolling circle replication (Bi et al., 2015; Cai et al., 2014; Hu et al. 2017, 2018a, 2018b; Kahn et al., 2015; Lawal, 2018; Lou et al., 2015; Qi et al., 2018; Ren et al., 2015; Sheng et al., 2015; Yan et al., 2017; Yue et al., 2019). Exo III is a universal signal amplification tool for constructing a universal detection platform because it does not require a specific recognition sequence (Zhang et al., 2013; Zou et al., 2011). Exo III can be used to gradually catalyze the hydrolysis of 3′ concave or blunt end of double-strand DNA (dsDNA) and, single-strand DNA (ssDNA), while the 3′ convex end in duplex is resistant to the action of the enzyme (Rogers and Weiss, 1980; Zou et al., 2011). Here, Exo III was chosen for recycling amplification because of its universality and excellent repeatability.

In this work, hybridization reaction and Exo III digesting were performed directly in solution. As shown in Scheme 1, two hairpin report DNAs that served as double signals were introduced to hybridize the target. After Exo III was added, the target and report fragments (ssDNA) were released. The resulting recycling and double-signals improve the accuracy and sensitivity of the sensor. In most research, the releasing report fragments were captured through hybridization with some DNA modified on the electrodes (Li et al. 2016b, 2017a); however, these techniques are relatively complicated. Simplifying modification of the electrode and the combination of the interface with the solution reaction can improve the stability and repeatability of the biosensor, and simplify the biosensor operation. Recent studies demonstrated that graphene preferentially binds to ssDNA than dsDNA via $\pi-\pi$ stacking (Li et al. 2015, 2016a, 2017b; Liu et al. 2008, 2013; Zhang et al., 2017). Thus, combining solution reactions to the graphene-modified interface was used in the biosensor. The released report fragments (ssDNA) are adsorbed selectively on the surface of the graphene-modified electrode to generate electrochemical signals. This novel strategy allows both sequence and length of repeats to be detected with high selectivity, accuracy, sensitivity, and stability. This biosensor has great potential as early warning and clinical diagnostic tools for neurodegenerative diseases.

## 2. Experimental section

### 2.1. Fabrication of electrochemical biosensor

First, GCE was polished with a 0.05 μm $Al_2O_3$ powder. After polishing, the electrodes were sonicated once in ethanol and twice in ultrapure water for 5 min, and the cleaned electrodes were dried at room temperature. Next, the graphene suspension in 5 μL of DMF was dropped on the electrode surface and dried at room temperature and stable humidity.

### 2.2. DNA hybridization and digestion process

First, target/H-Fc/H-MB complex was prepared by the hybridization reaction that was performed through different concentrations of target DNA, 3 μM of H-Fc (Ferrocene-labeled hairpin DNA), and 1 μM of H-MB (Methylene Blue-labeled hairpin DNA) at 90 °C for 5 min in water bath, followed by naturally cooling to room temperature. After addition of Exo III, the mixture was allowed to react at 37 °C for 80 min in a constant temperature incubator. The reaction system was terminated by heat treatment at 80 °C for 20 min. Finally, 3 μM S1 and 1 μM S2 DNA were added to hybridize with the remaining hairpin DNA to form a double strand at 80 °C for 5 min, followed by naturally cooling to room temperature. The hybridization reaction and enzymatic cleavage were studied by the 15% native polyacrylamide gel electrophoresis (Fig. S3) and electrochemical impedance spectroscopy (Fig. 1B and Fig. 1C). The details can be seen in supporting information.

## 3. Results and discussion

### 3.1. Design principle of the sensor

Several techniques, including ratiometric technique, Exo III-Assisted recycling and selective adsorption of graphene for ssDNA, were used to set up a novel electrochemical method (as shown in Scheme 1) for the detection of CAG trinucleotide repeat. Both concentration and repeat

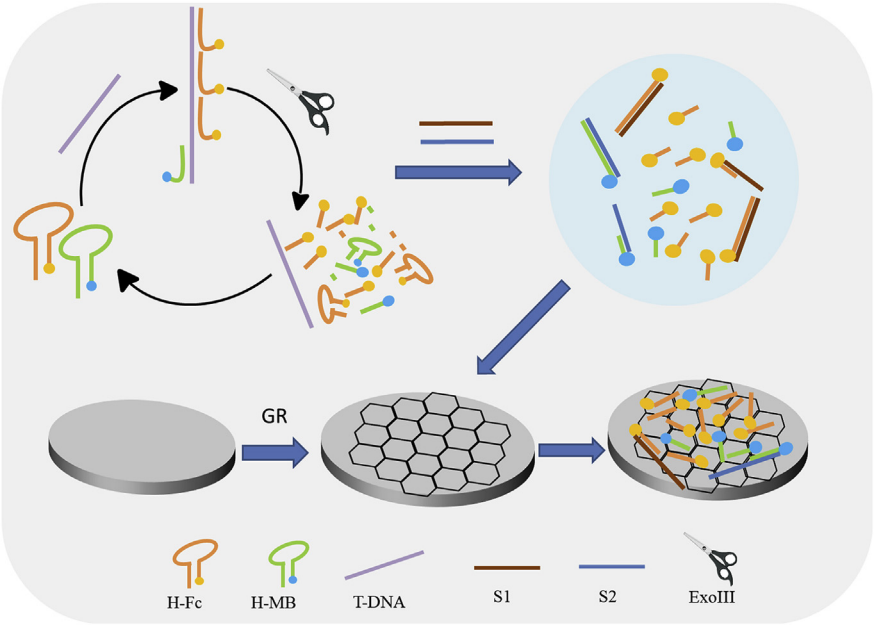


**Scheme 1.** Schematic diagram of a novel electrochemical biosensor based on double-signal technique, Exo III-Assisted Recycling and adsorption selectivity of graphene, for the detection of the trinucleotide repeat $d(CAG)_n$.

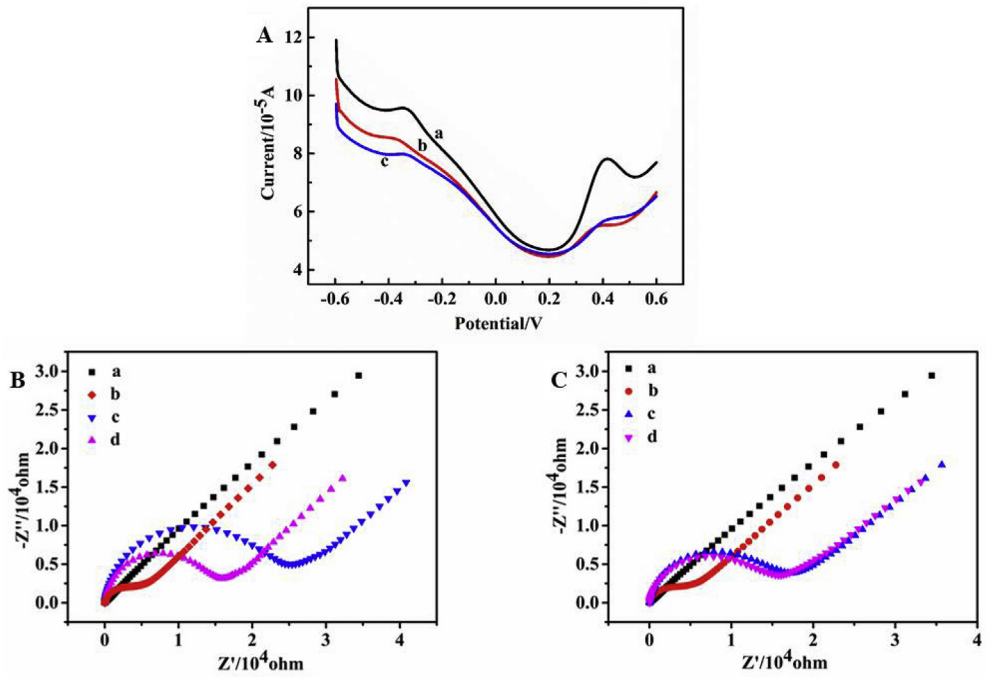


**Fig. 1.** (A). SWV response of the biosensor: (a) SWV curve of the sensor (target: 10 nM), (b) SWV curve of the sensor without target, (c) SWV curve of the sensor without Exo III. (B) EIS of DNA hybridization and enzymatic digestion (a) bare GE, (b) T-DNA|GE, (c) MCH|H1–H2|T-DNA|GE, (d) Exo III|MCH|H1–H2|T-DNA|GE; (C) EIS of DNA hybridization and enzymatic digestion without hairpin DNA (a) bare GE, (b) T-DNA|GE, (c) MCH|T-DNA|GE, (d) Exo III|MCH|T-DNA|GE.

number of the repeat DNA can be tested through the application of these techniques. The double-signal was based on the H-Fc DNA, H-MB DNA. The relative length of repeat may be calculated from the ratio of two kinds of electrochemical signal intensities: in the absence of target DNA, the hairpin DNAs would exist stably in their respective stem-loop configuration, while the hairpin DNAs were opened and hybridized with the target to produce double-strands with a blunt 3′-terminus in the presence of target DNA. In consideration of the high propensity of trinucleotide repeat DNA to form a stable hairpin structure, the hybridization reaction can't be done in normal hybridization condition according to our previous work (Li et al., 2017c). Thus, the hybridization was carried out at 90 °C for 5 min in water bath, followed by naturally cooling to room temperature.

An important problem is how to achieve these electrochemical signals efficiently and simply. Here, the Exo III-Assisted Recycling and adsorption selectivity of graphene were used to achieve this aim. Exo III cleavage process was triggered, accompanied by the autonomous release of the target DNA and report fragments (short ssDNA with Fc or MB: Fc-GCAGGCTA, MB-GCACACGCT). The released target DNAs can be continuously hybridized with H-Fc and H-MB to form duplex DNA. The target recycling would expand detection signals, and the signals of Fc and MB in the report fragments can be detected by the graphene-modified electrode that selectively adsorbed ssDNA. As shown in Fig. S1, in the presence of ssDNA labeled Fc (2 μM), the graphene electrode showed the highest electrochemical signal. However, the graphene electrode showed almost no signal in the presence of dsDNA labeled Fc (2 μM). Indeed, our data confirmed that the graphene-modified electrode can absorb ssDNA selectively. In addition, in the presence of hairpin DNA labeled Fc (2 μM), the graphene electrode also showed some current, meaning that hairpin DNA can also be absorbed by a certain amount, which indicates that the remaining hairpin DNA may affect the accuracy of detection (Fig. S2). In order to eliminate the signal of hairpin DNA, two ssDNA (S1 and S2) that were fully complementary pairing with hairpin DNA were introduced to form a duplex with the remaining hairpin DNA. The hairpin report DNA (H-Fc, H-MB) had been hybridized with S1 or S2 to form the duplex, which results in almost zero current (Fig. S1 curve c). In the sensor, the current values have a decrease because of the elimination of background signal after the treatment. As shown in Fig. S2, the electrochemical signals had some decrease because of the elimination of background signal, after the addition of S1 and S2 (Fig. S2). The unreacted hairpin report DNA (H-Fc: 3 μM, H-MB: 1 μM) had been hybridized with S1 (3 μM) or S2 (1 μM) to form the duplex.

### 3.2. Hybridization of DNA and detection effect of the biosensor

Hybridization is very key process for successful preparation of the biosensor (Nie et al., 2018; Xiong et al., 2015). The results of native polyacrylamide gel electrophoresis (PAGE) and electrochemical impedance spectroscopy (EIS) confirmed the excellent DNA hybridization reaction and digestion process. The detail discussion was seen in supporting information.

Another important issue concerns the electrochemical signal acquisition when CAG trinucleotide repeat was detected through H-Fc and H-MB DNA probes. In the presence of target DNA, the probe DNA would be opened, and formed duplex DNA with blunt 3′-terminus. Exo III triggered the cycle of target DNA and released free short ssDNA fragments labeled with Fc or MB, which could be adsorbed on the surface of the graphene-modified electrode, and which was certificated by the observed current (curve a in Fig. 1A). However, the hairpin report DNA could not be opened and maintained the original hairpin structure in the absence of repeat DNA. Consequently, no dsDNA with a blunt 3′-terminus can't be formed, which can't trigger the enzymatic cleavage process and release the short ssDNA fragments with electrochemical signals. Pleasantly, there was no obvious current in the absence of target, as shown at curve b in Fig. 1A. In the absence of Exo III, the sensor could not be activated, no free report fragments were released. Accordingly, no obvious current was observed (curve c in Fig. 1A). These results indicated that the strategy based on hybridization, Exo III recycling and selective adsorption of graphene is successful, and the biosensor can detect the target DNA. Furthermore, no current could be recorded in the presence of target when the electrode without graphene was used (curve a in Fig. S5). No current was also found when the modified-graphene electrode was used in the absence of target (curve b in Fig. S5).

### 3.3. Selectivity of the electrochemical sensor

High selectivity is one of the core elements of an efficient biosensor. To assess the specificity of the proposed method, several interfering gene sequences associated with neurodegenerative diseases were tested, including $d(CTG)_{15}$, $d(CCG)_{15}$, $d(GAA)_{15}$, $d(TGG)_{15}$, $d(CGG)_{15}$, and $d(ATT)_{15}$. A comparative study was performed by measuring a low concentration of target DNA (100 pM) and a high concentration of interfering species (1 nM). The amperometric responses of Fc for d $(CAG)_{15}$ repeat and other interfering DNA repeats were shown in Fig. S7. The highest current could be observed for $d(CAG)_{15}$ even if the concentration of $d(CAG)_{15}$ was only 1/10 times of interfering species. These results demonstrated the high selectivity of the proposed biosensor for $d(CAG)_{15}$ among the TNR biomarkers of neurodegenerative diseases.

### 3.4. Effect of target DNA on signals from ferrocene and methylene blue

The relationship between the output signals and target concentration was investigated for the quantitative detection of $d(CAG)_n$ TNRs. The double signals of the proposed biosensor were monitored at the different concentrations of $d(CAG)_{15}$ under the optimal experimental conditions. As shown in Fig. 2A, the currents of Fc and MB were gradually increased with the increasing concentrations of repeats from the curve a to f, indicating that both signal responses relied highly on the target concentrations. It was found that the plot of current change vs. The logarithm of $d(CAG)_{15}$ concentration exhibited a strong linear relationship from 1 pM to 100 nM (Fig. 2B and C). For ferrocene, the linear equation was $I = 1.948\ \lg c + 13.41$with a correlation coefficient of 0.998; the limit of detection (LOD) was calculated to be 0.27 pM in a 3s rule ($LOD = 3\sigma/k$, σ is the standard deviation of the blank and k is the slope of the corresponding calibration curve). For methylene blue, the linear equation was $I = 0.6649\ \lg c + 4.687$ with a correlation coefficient of 0.9992; the limit of detection (LOD) was calculated to be 0.22 pM in a 3s rule. These results showed that the biosensor had an admirable quantitative correlation with higher sensitivity and lower LOD in comparison with other DNA biosensors (Table S3).

Theoretically, the current ratio of ferrocene and methylene blue should be certain as the repeat number should be unchanged whatever concentrations of repeat DNA. Fortunately, the current ratio (F/M) of ferrocene and methylene blue was very much stable at different target concentrations based on our data as shown in Fig. 2D. The result indicated that the current ratio (F/M) had no correlation with $d(CAG)_n$ concentrations, which provided strong experimental basis for next further correlation research of repeat length and current signals.

### 3.5. The correlation of repeat numbers and current signals

For TNR biomarker of neurodegenerative diseases, different lengths of TNR led to different disease severity. Once the threshold repeat length reached, the disease symptoms would appear. The numbers of repetitions are crucial for diagnosing neurodegenerative diseases. Therefore, the study of the relationship between numbers of repetitions (n value) and current signals is essential. However, rapid detection methods of TNR sequence lengths, such as sequencing and gel electrophoresis, have not attracted much attention because their special structure rendered the detection behavior more difficult.

In this study, the ratiometric biosensor was specifically designed to determine more reliable numbers of repetitions. Under the optimal experimental conditions, $d(CAG)_n$ trinucleotide repeat (1 nM) with different repeat numbers was used to study the correlation (Fig. S8). Based on the principle of the biosensor, one strand of the target only binds to one strand of H-MB. Thus, the currents of MB remained relatively constant with increasing n because of the same concentrations of

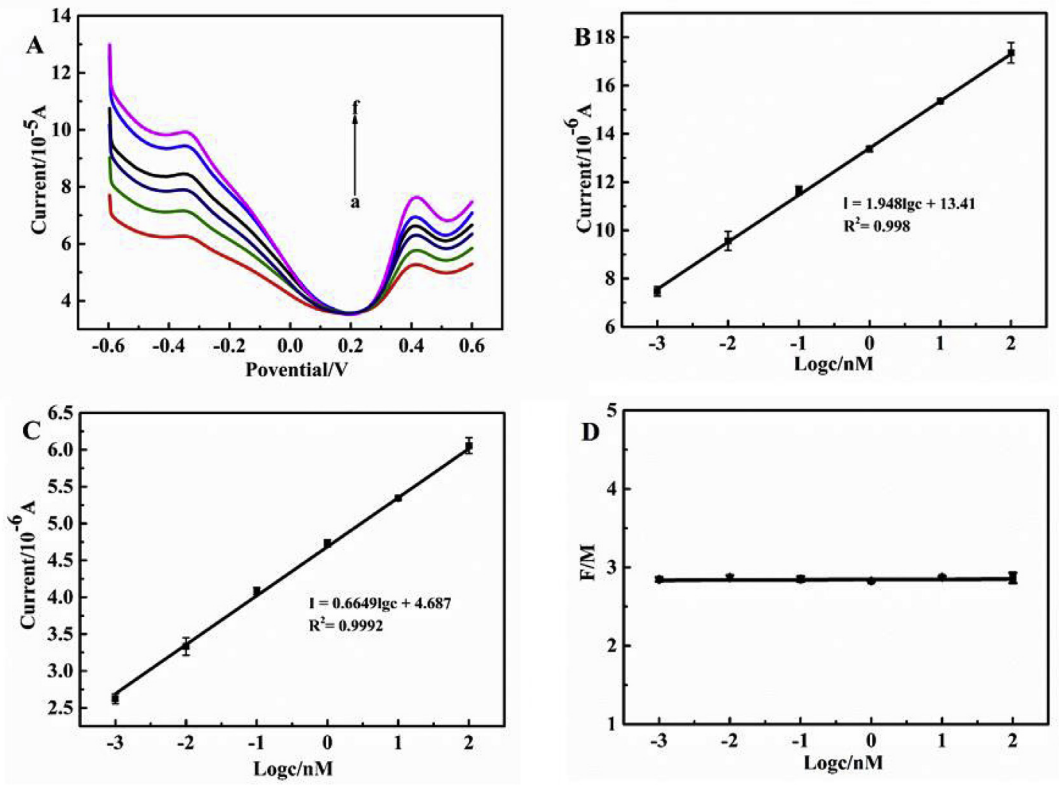


**Fig. 2.** (A) Current responses of the electrode incubated with different $d(CAG)_{15}$ trinucleotide repeats concentrations in PBS (pH = 7.4) (from a to f: 0.001, 0.01, 0.1, 1, 10, 100 nM); (B) The calibration plots of Fc current versus the logarithm concentration of $d(CAG)_{15}$ trinucleotide repeats; (C) The calibration plots of MB current versus the logarithm concentration of $d(CAG)_{15}$ trinucleotide repeats. The error bars represent the standard deviation of three measurements. (D) The ratio of two signals (F/M) in different concentrations of $d(CAG)_{15}$ trinucleotide repeats.

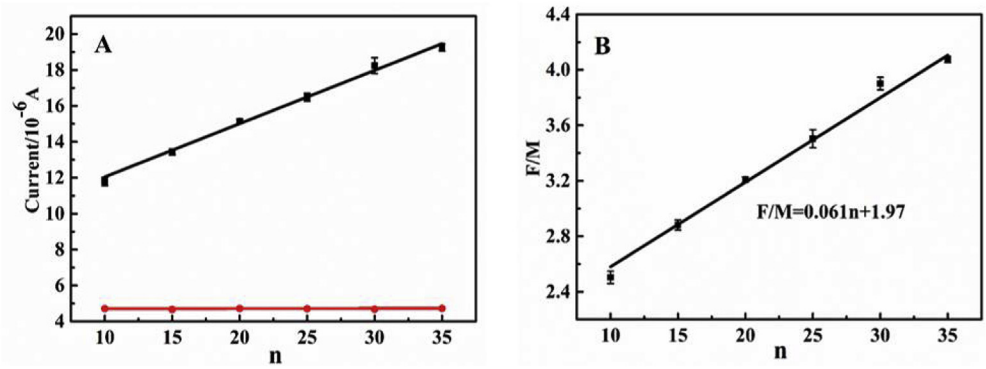


**Fig. 3.** (A) The current responses of F signal and M signal when different repeat number was detected (black line: Fc, red line: MB); (B) The corresponding linear curves of ratio of the electrode incubated with different number of n of CAG trinucleotide repeat in PBS (pH = 7.4) (n = 10, 15, 20, 25, 30, 35). The average of three samples was studied. (For interpretation of the references to colour in this figure legend, the reader is referred to the Web version of this article.)

DNA, as shown in Fig. 3A. Meanwhile, target DNA can bind with more strands of H-Fc, even when repeat numbers increased at the same target concentration. It was found that the current signal of ferrocene had increased with the repeat numbers increasing from 10 to 35 with excellent linearity. The linear equation was I = 0.2966 n + 9.081, with a correlation coefficient of 0.993, where n is length of the repeat of CAG trinucleotide.

The determination of n value of repeats is crucial. Although the linear correlation between Fc and n was excellent, the current of Fc also changed with difference of the target concentrations. It is unreliable and unscientific if one signal variable was only used to determine n value. Based on the above discussions, we employed the ratio F/M to determine the n value as it is almost a constant for the same repeat with different concentrations (Fig. 2D). As shown in Fig. 3B, an excellent linear relationship between F/M and n was observed with a correlation coefficient of 0.992 (the equation was F/M = 0.061 n+1.97). Note here that the equation is invalid when n value is less than 5, because there is a low chance that H-Fc hybridizes with the target. Other concentration of the target was also used to demonstrate further that the ratio of both signals (F/M) has no significant relationship with the target concentration. It was found that the obtained results were almost consistent (Figs. S9 and S10). Reasonably, the number of TNR was reliably obtained from measurements of F/M via this double-signal technique: such a simple, rapid, and the inexpensive electrochemical sensor is, thus, extremely useful for the early diagnosis of neurodegenerative diseases.

### 3.6. Application of the sensor to real samples

To further assess the applicability of the novel electrochemical sensor in real samples, we determined d$(CAG)_n$ TNRs samples in human serum. A series of samples were prepared by adding d$(CAG)_n$ repeats with different concentrations and n values in 10-fold-diluted human serum (obtained from ZiJing Hospital of Wuhan, Hubei Province). Then, the concentrations and n values of the targets were determined via the novel sensor. First, n value was determined by the ratio F/M based on the above described linearity relationship. As shown in Table 1, the obtained n values based on the method are quite accurate. The relative standard deviations (RSDs) were in the range of 2.2%–3.2%, while the recoveries were from 95.4% to 103%. Furthermore, we randomly chose another concentration(100 pM)for the test

**Table 1**
Detection different repeat number of CAG trinucleotide repeats (1 nM) added in human serum (n = 3).

| Sample | n value of d$(CAG)_n$/1 nM | signal | Found n value | RSD% | Recovery% |
|---|---|---|---|---|---|
| 1 | 15 | F/M | 14.31 | 2.2 | 95.4 |
| 2 | 25 | F/M | 25.72 | 2.5 | 103 |
| 3 | 35 | F/M | 34.17 | 3.2 | 97.6 |

**Table 2**
Detection of different concentrations $(CAG)_{15}$ added in human serum (n = 3).

| Sample | Added concentration of d$(CAG)_{15}$/nM | signal | Found concentration/nM | RSD% | Recovery% |
|---|---|---|---|---|---|
| 1 | 0.1 | MB | 0.11 | 2.2 | 110 |
| | | Fc | 0.10 | 4.1 | 100 |
| 2 | 1 | MB | 1.03 | 1.8 | 103 |
| | | Fc | 0.93 | 2.8 | 93.0 |
| 3 | 10 | MB | 9.46 | 1.9 | 94.6 |
| | | Fc | 9.63 | 1.9 | 96.3 |

(Table S2); the recoveries ranged from 98.3% to 101%, and the RSDs were in the range of 3.7%–4.2%, respectively. These results indicated that the repeat length can be determined accurately by the ratio (F/M) even in a complex biological environment as the test was not affected by target concentration. Moreover, the concentration of targets can be detected by any signal of both Fc and MB. As shown in Table 2, the detected concentrations were consistent regardless of Fc or MB. The RSDs were in the range of 1.9%–4.1%, the recoveries were from 93% to 100%. These outcomes confirmed that the sensor can be applied for the detection of repeat length and sequence in complex biological environment, indicating that the novel biosensor is an excellent potential tool for early diagnosis of neurodegenerative diseases.

## 4. Conclusions

In this work, we designed a novel ratiometric electrochemical sensor with excellent specificity and sensitivity for the detection of d$(CAG)_n$ trinucleotide repeats. The biosensor was constructed mainly based on ratiometric technique, Exo III-Assisted target recycling and adsorption selectivity of graphene for ssDNA. An excellent linear relationship was observed between the electrochemical signal and the concentration of d$(CAG)_n$ repeats in the range from 1 pM to 100 nM with a LOD as low as 0.22 pM. Importantly, the signal ratio, F/M, is used as the metric for determining reliable repeat numbers, which are independent of target concentrations. The linear equation F/M = 0.061 n + 1.97 (n = 10–35) was obtained with a correlation coefficient of 0.992. Furthermore, the tests of repeat numbers and concentrations can be performed in complexed human serum, indicating the potential of this novel biosensor for the early diagnosis of neurodegenerative diseases. This new ratiometric electrochemical biosensor provides a feasible strategy to determine the sequence and repeats length of trinucleotide repeats in clinical applications. Furthermore, some advantages of the biosensor, including double-signal technique, direct hybridization in solution with dependent of electrode interface and excellent selectivity, render the method simple and feasible even for non-professional operators.

## Declaration of competing interest

The authors declare that they have no known competing financial interests or personal relationships that could have appeared to influence the work reported in this paper.

## CRediT authorship contribution statement

**Yalan Liu:** Writing - original draft, Formal analysis. **Zhiqi Ge:** Formal analysis. **Meijun Chen:** Formal analysis. **Hanping He:** Funding acquisition, Investigation, Methodology, Project administration. **Xiuhua Zhang:** Formal analysis. **Shengfu Wang:** Formal analysis.

## Acknowledgments

This work was supported by National Natural Science Foundation of China (21575035), and Foreign Science and Technology Cooperation Fund of Hubei province, China (2015BHE025).

## Appendix A. Supplementary data

Supplementary data to this article can be found online at https://doi.org/10.1016/j.bios.2019.111537.

## References

Bi, S., Jia, X., Ye, J., Dong, Y., 2015. Biosens. Bioelectron. 71, 427–433.
Cai, Z., Chen, Y., Lin, C., Wu, Y., Yang, C.J., Wang, Y., Chen, X., 2014. Biosens. Bioelectron. 61 (21), 370–373.
Dürr, A., Cossee, M., Agid, Y., Campuzano, V., Mignard, C., Penet, C., Mandel, J.-L., Brice, A., Koenig, M., 1996. N. Engl. J. Med. 335 (16), 1169–1175.
Evansgalea, M.V., Hannan, A.J., Carrodus, N., Delatycki, M.B., Saffery, R., 2013. Trends Mol. Med. 19 (11), 655–663.
Fojta, M., Havran, L., Kizek, R., Billova, S., Palecek, E., 2005. Biosens. Bioelectron. 20 (5), 985–994.
Fojta, M., Havran, L., Marie Vojtiskova, A., Palecek, E., 2004. J. Am. Chem. Soc. 126 (21), 6532.
Fu, YingHui, Kuhl, Derek, P.A., Pizzuti, Antonio, Pieretti, Maura, Sutcliffe, James, S., 1991. Cell 67 (6), 1047–1058.
He, H., Peng, X., Huang, M., Chang, G., Zhang, X., Wang, S., 2014. Analyst 139 (21), 5482–5487.
He, H., Xia, J., Peng, X., Chang, G., Zhang, X., Wang, Y., Nakatani, K., Lou, Z., Wang, S., 2013. Biosens. Bioelectron. 49, 282–289.
Hu, Q., Wang, Q., Jiang, C., Zhang, J., Kong, J., Zhang, X., 2018a. Biosens. Bioelectron. 110, 52–57.
Hu, Q., Wang, Q., Kong, J., Li, L., Zhang, X., 2018b. Biosens. Bioelectron. 101, 1–6.
Hu, Q., Wang, Q., Sun, G., Kong, J., Zhang, X., 2017. Anal. Chem. 89 (17), 9253–9259.
Kahn, J.S., Trifonov, A., Cecconello, A., Guo, W., Fan, C., Willner, I., 2015. Nano Lett. 15 (11), 7773.
Kannan, B., Williams, D.E., Booth, M.A., Travas-Sejdic, J., 2011. Anal. Chem. 83 (9), 3415–3421.
Kremer, B., Goldberg, P., Andrew, S.E., Theilmann, J., Telenius, H., Zeisler, J., Squitieri, F., Lin, B., Bassett, A., Almqvist, E., 1994. N. Engl. J. Med. 330 (20), 1401–1406.
López Castel, A., Cleary, J.D., Pearson, C.E., 2010. Nat. Rev. Mol. Cell Biol. 11, 165.
La Spada, A.R., Wilson, E.M., Lubahn, D.B., Harding, A.E., Fischbeck, K.H., 1991. Nature 352 (6330), 77–79.
Lange, K.J., Mcinnis, M.G., 2002. CNS Spectr. 7 (3), 196–202.
Lawal, A.T., 2018. Biosens. Bioelectron. 106, 149–178.
Li, B., Pan, G., Avent, N.D., Lowry, R.B., Madgett, T.E., Waines, P.L., 2015. Biosens. Bioelectron. 72, 313–319.
Li, C., Lu, W., Zhu, M., Tang, B., 2017a. Anal. Chem. 89 (20).
Li, F., Liu, X., Zhao, B., Yan, J., Li, Q., Aldalbahi, A., Shi, J., Song, S., Fan, C., Wang, L., 2017b. ACS Appl. Mater. Interfaces 9 (18), 15245.
Li, J., Liu, Y., Zhu, X., Chang, G., He, H., Zhang, X., Wang, S., 2017c. ACS Appl. Mater. Interfaces 9 (50), 44231.
Li, L., Feng, J., Liu, H., Li, Q., Tong, L., Tang, B., 2016a. Chem. Sci. 7 (3), 1940–1945.
Li, Y., Zhao, Q., Wang, Y., Man, T., Lu, Z., Xu, F., Hao, P., Chi, L., Jian, L., 2016b. Anal. Chem. 88 (23), 11684–11690.
Lin, M., Wang, J., Zhou, G., Wang, J., Wu, N., Lu, J., Gao, J., Chen, X., Shi, J., Zuo, X., 2015. Angew. Chem. Int. Ed. 127 (7), 2179–2183.
Liu, X., Wang, F., Aizen, R., Yehezkeli, O., Willner, I., 2013. J. Am. Chem. Soc. 135 (32), 11832–11839.
Liu, Y., Li, J., Chang, G., Zhu, R., He, H., Zhang, X., Wang, S., 2018. New J. Chem. 42 (12), 9757–9763.
Liu, Z., Robinson, J.T., Sun, X., Dai, H., 2008. J. Am. Chem. Soc. 130 (33), 10876–10877.
Lou, J., Wang, Z., Wang, X., Bao, J., Tu, W., Dai, Z., 2015. Chem. Commun. 51 (78), 14578–14581.
Mirkin, S.M., 2007. Nature 447 (7147), 932–940.
Mitchell, J.E., Newbury, S.F., Mcclellan, J.A., 1995. Nucleic Acids Res. 23 (11), 1876.
Nie, J., Yuan, L., Jin, K., Han, X., Tian, Y., Zhou, N., 2018. Biosens. Bioelectron. 122, 254–262.
Qi, H., Yue, S., Bi, S., Song, W., Ding, C., 2018. Sens. Actuators B Chem. 273, 1525–1531.
Ranen, N.G., Stine, O.C., Abbott, M.H., Sherr, M., Codori, A.M., Franz, M.L., Chao, N.I., Chung, A.S., Pleasant, N., Callahan, C., 1995. Am. J. Hum. Genet. 57 (3), 593–602.
Ren, W., Gao, Z.F., Li, N.B., Luo, H.Q., 2015. Biosens. Bioelectron. 63 (4), 153–158.
Rogers, S.G., Weiss, B., 1980. Methods Enzymol. 65 (1), 201–211.
Sheng, Q., Cheng, N., Bai, W., Zheng, J., 2015. Chem. Commun. 51 (11), 2114–2117.
Snow, K., Doud, L.K., Hagerman, R., Pergolizzi, R.G., Erster, S.H., Thibodeau, S.N., 1993. Am. J. Hum. Genet. 53 (6), 1217–1228.
Stevens, J.R., Lahue, E.E., Li, G.M., Lahue, R.S., 2013. Cell Res. 23 (4), 565–572.
Suen, I.S., Rhodes, J.N., Christy, M., Mcewen, B., Gray, D.M., Mitas, M., 1999. BBA-Gene. Struct. Expr. 1444 (1), 14–24.
Sutherland, G.R., Richards, R.I., 1995. Proc. Natl. Acad. Sci. 92 (9), 3636.
Xiong, E., Zhang, X., Liu, Y., Zhou, J., Yu, P., Li, X., Chen, J., 2015. Anal. Chem. 87 (14), 7291–7296.
Yan, Y., Yue, S., Zhao, T., Luo, B., Bi, S., 2017. Chem. Commun. 53 (90).
Yu, A., Dill, J., Wirth, S.S., Huang, G., Lee, V.H., Haworth, I.S., Mitas, M., 1995. Nucleic Acids Res. 23 (14), 2706–2714.
Yue, S., Song, X., Song, W., Bi, S., 2019. Chem. Sci. 10 (6), 1651–1658.
Zühlke, C., Atici, J., Martorell, L., Gembruch, U., Kohl, M., Göpel, W., Schwinger, E., 2015. Prenat. Diagn. 20 (1), 66–69.
Zhang, H., Li, F., Dever, B., Li, X.F., Le, X.C., 2013. Chem. Rev. 113 (4), 2812–2841.
Zhang, H., Zhang, H., Aldalbahi, A., Zuo, X., Fan, C., Mi, X., 2017. Biosens. Bioelectron. 89, 96–106.
Zhu, X., Li, J., Lv, H., He, H., Liu, H., Zhang, X., Wang, S., 2017. RSC Adv. 7 (57), 36124–36131.
Zou, B., Ma, Y., Wu, H., Zhou, G., 2011. Angew. Chem. Int. Ed. 123 (32), 7533–7536.